Is the Use of Underwater Polarized Light by Fish Restricted to Crepuscular Time Periods?

IÑIGO NOVALES FLAMARIQUE*†, CRAIG W. HAWRYSHYN*

We measured the spectral distributions of the underwater total and polarized light fields in the upper photic zone of meso-eutrophic waters (i.e., blue–green waters containing medium to high chlorophyll a concentrations). Per cent polarization levels during the day were always lower than 40%, but at crepuscular times these values could increase to 67%. A corresponding change occurred in the spectral distribution, with proportionately more shorter wavelength photons contributing to the total spectrum during crepuscular periods. Electrophysiological recordings from the optic nerve of rainbow trout subjected to light stimuli of varying polarization percentages show that the animal's threshold for detecting polarized light is between 63 and 72%. These physiological findings suggest that the use of water-induced polarized light cues by rainbow trout and similar percomorph fish should be restricted to crepuscular time periods. © 1997 Elsevier Science Ltd. All rights reserved.

Polarized light   Vision   Crepuscular   *Oncorhynchus mykiss*

INTRODUCTION

Sunlight reaching the Earth's atmosphere is unpolarized, i.e., there is no preferential plane in which the electric field of most photons oscillates. However, when individual photons interact with various components of the atmosphere and water column, a scattering phenomenon takes place, which was first described by Lord Rayleigh (Rayleigh, 1889). In the water, Rayleigh scattering is caused by molecular and particle scattering. In the sky, Rayleigh scattering arises from minute density fluctuations in the atmosphere caused by changes in temperature. These fluctuations create microirregularities in the refractive index of the medium through which the light travels. If the physical scale of the irregularities is smaller than about 1/10th of the wavelength of the incident light, the resulting radiation pattern is a toroid around the scattering dipole (Hecht & Zajac, 1974). Rayleigh scattering produces scattered light which is 100% polarized at right angles to the incident unpolarized beam. It is this, as well as other natural phenomena leading to polarization of sunlight (see Hecht & Zajac, 1974), that are exploited by animals capable of differentiating between individual planes of light. Such animals are sensitive to the direction and amplitude of the electric field (E-vector) of polarized light.

Polarization sensitivity was first documented for the honey bee in the late 1940s (von Frisch, 1949). Since this early pioneering work, other invertebrates, terrestrial and aquatic, as well as fish, amphibians and birds have been shown to at least exhibit polarotactic responses (for reviews see Waterman, 1981, 1984). Nevertheless, it is only for the desert ant (*Cataglyphis bicolor*), the cricket (*Grillus campestris*) and the honey bee (*Apis apis*) that thorough descriptions linking the anatomical features and neurophysiological mechanisms underlying the animal's use of polarized light are well documented (Wehner, 1983, 1989; Labhart, 1988, 1996). Work with vertebrates, by comparison, is at an early stage (Coughlin & Hawryshyn, 1995).

Most polarized light investigations with vertebrates have used fish as study subjects (Waterman, 1981; Cameron & Pugh, 1991; Parkyn & Hawryshyn, 1993). This choice, although satisfactory due to the potential for visual diversity from the richness of photic environments that fish inhabit, nonetheless makes implications for the behaviour and life strategies of the animal hard to discern. Indeed, it is difficult to follow a fish in its natural habitat and to isolate the effect that a particular variable, such as polarized light, has on its behaviour. As a consequence, our knowledge of polarized light sensitivity in vertebrates is restricted to responses under laboratory settings which may not be representative of the natural environment of the animal. This restricted knowledge also applies to the characterization of the natural underwater polarized light field that would permit the observed laboratory behaviours in nature.

Since the first observations of polarized light in the ocean (Waterman, 1954), a magnificent body of experimental work has been carried out by various researchers

*University of Victoria, Department of Biology, P.O. Box 3020, Victoria, BC, V8W 3N5, Canada.
†To whom all correspondence should be addressed [Fax: +1-250-721-7120; Email: inovales@uvvm.uvic.ca].

FIGURE 1. Geometrical definitions of variables used in the text (modified from Timofeeva, 1974). See also Table 1.

maximum polarization). From this past work, it was concluded that per cent polarization was highest for solutions with the biggest absorption and lowest dispersion coefficients, regardless of the source's azimuth direction (Timofeeva, 1961). In accordance with these observations, the regions of the spectrum least absorbed in laboratory solutions and in the ocean were also the least polarized (Timofeeva, 1962; Ivanoff & Waterman, 1958). Timofeeva also studied the dependence of the degree of polarization and direction of E-max on azimuth angle of the light source and direction of observation (Timofeeva, 1969, 1974). Results from these studies proved the existence of submarine neutral points in the plane of the sun (Timofeeva, 1974), and explained E-max and per cent polarization trends observed for all azimuth planes (Timofeeva, 1962; Ivanoff & Waterman, 1958; Waterman & Westell, 1956). Further work by this and other authors also revealed a negative relationship between per cent polarization and increasing depth (Timofeeva, 1974; Ivanoff & Waterman, 1958; Waterman & Westell, 1956; Waterman, 1955).

Although the underwater polarized light field has been thoroughly studied in the past, the application of these findings to animal visual systems requires further measurements. In particular, previous studies did not describe the polarized light field in the ultraviolet (UV) range (wavelengths <400 nm) (Ivanoff & Waterman, 1958; Timofeeva, 1962), yet the UV photoreceptor in many invertebrates and most fish (Hawryshyn & McFarland, 1987; Parkyn & Hawryshyn, 1993) is involved in polarized light sensitivity. Published measurements were also for individual wavelengths, or for the integrated spectrum from 400 to 700 nm, without showing the spectral distribution of the energy. Yet, activation of individual photoreceptors is a wavelength-dependent process dictated by the absorption properties of the photopigments (Govardovskii, 1976). Hence, the measurements presented in this study improve on previous ones by incorporating the spectrum from 300 to 400 nm and by showing the energy distribution for the expanded spectrum from 300 to 850 nm. In addition, our measurements show the dependence of the polarized light field on additional variables such as the time of day and different atmospheric and water conditions. We also

to characterize the underwater polarized light field and to determine the biological and physical factors controlling it (see Ivanoff, 1974; Loew & McFarland, 1990). The most complete description of underwater polarization combining laboratory and field measurements was given by Timofeeva (Timofeeva, 1961, 1962, 1969, 1974). In accordance with this author's work (Timofeeva, 1974), we describe our results using previous notation (Fig. 1, Table 1).

The physical parameters controlling the degree and E-max orientation of polarized light arising from underwater scattering were investigated by Timofeeva in the laboratory using "milky" solutions (Timofeeva, 1961, 1969, 1974; the E-max plane of a light source is the oscillation plane for the majority of electric fields from photons comprising the light source, it is the plane of

TABLE 1. Definitions of variables shown in Fig. 1

J = Elevation of the sun ($0° \leq J \leq 90°$)
n = Normal to a calm water surface
N = Nadir (straight down on $z–y$ plane)
OB = E-max vector
OC = Reference line (0 or 180 deg) on spectroradiometer radiance cone collector
OP = Long axis of spectroradiometer, the plane containing the light ray and OP is the scattering plane
r = Angle of refraction (on $z–y$ plane)
Z = Zenith (straight up on $z–y$ plane),
ψ = E-max angle (angle between the reference line OC and the E-max vector ($0° \leq \psi \leq 180°$)) E-min = E-max + 90 deg
ϕ = Azimuth angle (angle between the vertical plane through the light source and the vertical plane through OP containing the point in space viewed, angle AOM is in the $x–y$ plane)
θ = Zenith angle, angle from zenith direction ($\angle$ ZOP)
percent (%) polarization = (rad(E-max) − rad(E-min))/(rad(E-max) + rad(E-min)), where rad = radiance

provide the first polarized light measurements in a lake, an important set of data since most polarized light sensitive fish species documented are fresh water (Hawryshyn & McFarland, 1987; Cameron & Pugh, 1991; Parkyn & Hawryshyn, 1993; Coughlin & Hawryshyn, 1995).

The purpose of this study was, therefore, 2-fold: (i) to describe the spectral and polarized light fields in meso-eutrophic waters inhabited by polarized light sensitive fish species such as rainbow trout (*Oncorhyncus mykiss*), and to assess whether the light cues required for the observed laboratory behaviours (Hawryshyn et al., 1990; Hawryshyn & Bolger, 1990; Cameron & Pugh, 1991; Parkyn & Hawryshyn, 1993) are present in nature; and (ii) to reproduce the natural spectral background conditions in laboratory experiments in order to test the visual capabilities of the animal in nearly natural light settings. Although the data are interpreted in relation to the visual system of young rainbow trout, the characteristics of the light field can be used to assess the broader possibility of polarized light utilization by other aquatic organisms.

MATERIALS AND METHODS

Measuring the polarized light field

The equipment used for the light measurements consisted of two major components: an LI-1800 underwater spectroradiometer (Biggs, 1984) and a rotatable column [Fig. 2(A–D)]. The column was made of 3 m pieces of plastic ABS pipe linked together with T connections by means of screws [Fig. 2(C, D)]. By releasing and re-tightening the top T screws at a certain depth of water, the length of column above it could be rotated through 360 deg in the x–y plane (Fig. 1). The spectroradiometer was fastened to the middle part of the T, and in the same fashion, it too could be rotated through 360 deg in the y–z plane. Combining these two axes permitted a scan to be taken in any direction within the allowed depths by the column (every 3 m). The column was secured by a heavy cement block at the bottom of the lake/ocean, and extended up to 1 m from the surface where a partially submerged buoy provided a surface fix for the column [Fig. 2(D)]. These attachments at both ends maintained the column upright and stable even under powerful ocean swells. The column, once installed, was maintained on the spot for the duration of the study. Only when a different water body was studied was the column repositioned.

The spectroradiometer apparatus could be modified for different types of light measurements by addition of various accessories [Fig. 2(A), Table 1]. To control the zenith angle θ, a metal protractor with 1 deg delineations was fastened on top of the spectroradiometer. By rotating the arm of the protractor a specific angle (corresponding to θ) could be selected [the protractor arm holds the level and compass in Fig. 2(A), it rotates from 0 to 180 deg in the y–z plane irrespective of spectroradiometer rotation]. The angle θ could then be set by rotating the spectroradiometer until the level built onto the rotatable arm
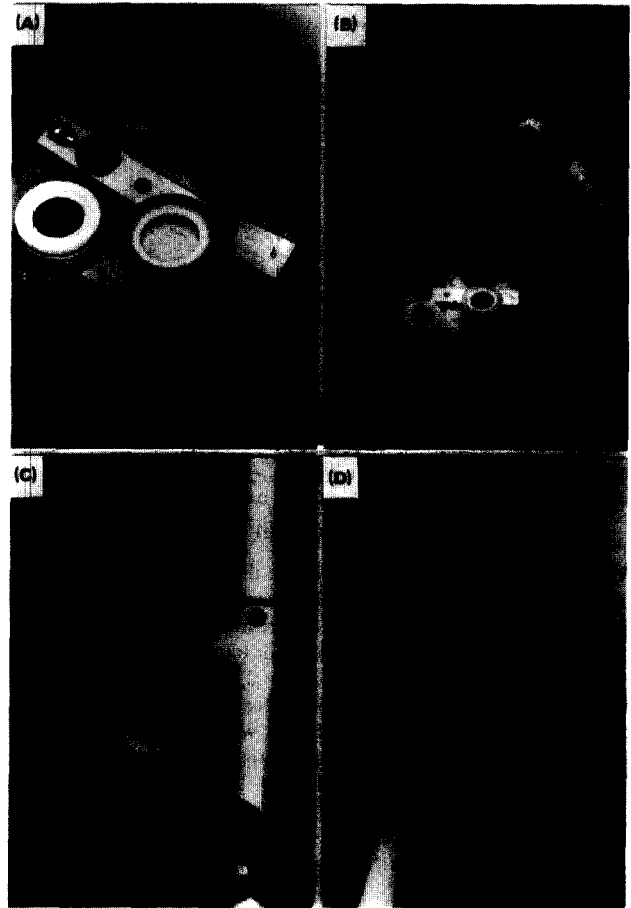
FIGURE 2. (A) Spectroradiometer (Spec) and associated equipment to measure the light field underwater. Lev, level; Comp, compass; Pro, protractor; E-vf, E-vector finder (polarization axis finder); Rc, radiance cone collector; Coc, Column connector; Col, column. (B) View of spectroradiometer 1.5 m below the ocean surface. Notice the multitude of speckles on the photograph indicating high numbers of particles in meso-eutrophic waters. (C) Diver searching for E-max, arrows indicate rotational joints and the planes of rotation on spectroradiometer-column system. (D) View of column with spectroradiometer attached.

indicated evenness in the x–y plane. A compass, located on the rotatable arm specified the azimuth angle φ. Without any other accessory, the spectroradiometer was ready to take spectral irradiance readings. To measure radiance, a solid cone holding a 30 deg angle aperture was placed over the cosine collector. This aperture was chosen because it is within the range of numerical apertures (30–45 deg) measured for parr rainbow trout eyes (Novales Flamarique, 1993). The cone was painted in black externally so that no stray light could reach the cosine collector. If polarized light readings were to be taken, a UV-grade linear polarizer transmissive from 300 to 850 nm (Polaroid HNP'B) was inserted into the top part of the cone. This polarizer could rotate over 180 deg, the delineations for which were engraved on the side of the cone in 1 deg intervals. To select the plane of maximum polarization (E-max), the diver looked through a polarization axis finder (Edmund Scientific) and transferred the angle read to the polarizer on the cone [Fig. 2(C)]. Both polarization axis finder and cone
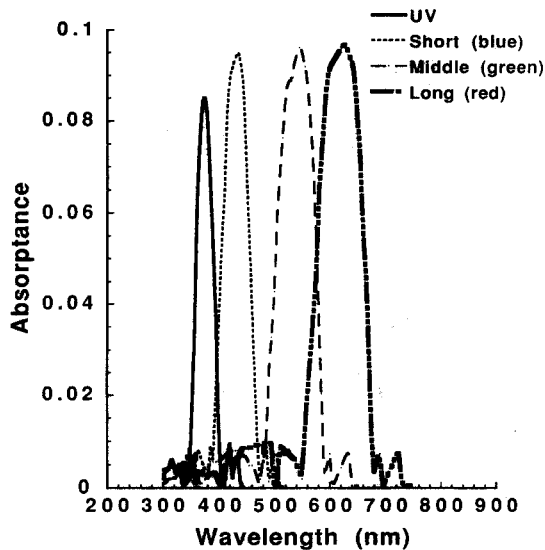
FIGURE 3. Absorptance spectra for the different cone photoreceptor mechanisms in rainbow trout. The ranges used for integrations correspond to the α peaks of the different cone absorbance spectra: 300–450 nm (UV), 340–520 nm (short or blue), 400–640 nm (middle or green) and 440–700 nm (long, or red, wavelength mechanism). Integration values were also computed for the β bands of the middle (300–400 nm) and long (320–420 nm) wavelength mechanisms. β band integrations are useful for comparison with laboratory results involving only UV light in the stimulus. In nature, the animal most likely uses mainly green and red light for visual processes involving double cones (which are green and red sensitive), and UV light for UV cones, whether the light is polarized or not.

time to complete a scan was approximately 35 sec. Scans were taken at different times of the day in various azimuth planes at depths ranging from 10 to 1 m below the surface. Parallel studies were conducted in Lake Cowichan and Ogden Point Breakwater (Vancouver Island, British Columbia, Canada). Both of these types of waters exhibit similar spectral irradiance characteristics (Novales Flamarique et al., 1992; Novales Flamarique & Hawryshyn, 1993).

Mathematical treatment of light measurements

To make the data meaningful in terms of salmonid vision, the loss of light before the rays encounter the fish retina, as well as the wavelength-dependent absorption of the four types of cone pigments found in young rainbow trout (UV, short (blue), middle (green) and long (red)-sensitive), had to be considered (Novales Flamarique & Hawryshyn, 1993). Thus the raw data were multiplied by transmission coefficients giving the percentage of light that would traverse the lens, cornea and vitreous fluid of the eye (Hawryshyn et al., 1989), and by the absorptance values of the cone photoreceptors examined. To obtain the absorptance values (Fig. 3), the pigment absorbance spectra, derived from an eighth order polynomial template for vertebrate cone absorption (Bernard, 1987) using MSP-obtained wavelength maxima, were first multiplied by the specific absorbance (0.0124/μm; Hárosi, 1975) and then by the average photoreceptor outer segment length in retinas of 12 g rainbow trout ($\sim$10 μm). Absorptance values were then calculated using the equation:

$$\text{Absorptance} = 1 - 10^{(-\text{absorbance})}.$$

Integrating the products of the absorptance values for each cone photoreceptor type and radiance values throughout any part of the spectrum thus indicated how much light was available to stimulate each cone type in that part of the spectrum. These results could then be compared to average radiance values that elicit fish

polarizer were sandwiched between two UV transmissive acrylite sheets (OP-4, Cyro Canada) and the degree delineations and directions of observation were the same for the cone and the polarization axis finder holder. All the parameters read were transferred to the boat-tender researcher using a two-way diver-to-boat communication system (Ocean Technology). The spectroradiometer was connected to a computer on the boat. Scans from 300 to 850 nm, every 5 nm, were taken upon diver signal. The

TABLE 2. Representative chlorophyll concentrations for May and June 1993 in Lake Cowichan and Ogden Point Breakwater

Depth (m)	LC (15 May 1993)				OPG (23 May 1993)			
	Chla	Chlb	Chlc	Phaeo	Chla	Chlb	Chlc	Phaeo
1	4.53	1.17	1.34	0.076	5.71	1.12	3.21	0.082
4	6.23	1.12	1.73	0.124	4.93	1.24	2.45	0.344
7	3.94	0.523	1.41	0.231	3.03	0.927	1.96	0.171
	LC (20 June 1993)				OPG (28 June 1993)			
1	2.21	1.02	1.29	0.607	5.02	1.65	2.94	0.122
4	2.94	1.31	1.03	0.128	2.38	1.09	1.67	0.138
7	6.34	1.42	1.96	0.342	2.26	0.847	1.13	0.067

LC, Lake Cowichan; OPG, Ogden Point Breakwater; Chla,b,c, chlorophyll a,b,c; Phaeo, phaeopigment (in mg/ml), $n = 3$ replicates, all standard errors <30% of value. Oligotrophic waters are characterized by 0.3 mg/ml < [Chla] < 3 mg/ml and appear blue; mesotrophic waters are greener and have typically 2 mg/ml < [Chla] < 15 mg/ml; eutrophic waters are dark green and show 10 mg/ml < [Chla] < 500 mg/ml. At either end of this spectrum are ultra-oligotrophic and hypereutrophic waters exhibiting extremely low and high Chla concentrations, respectively.
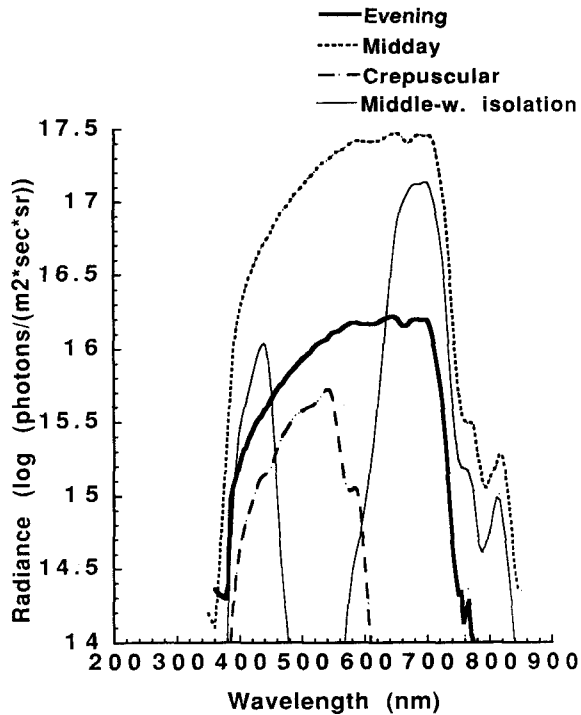
FIGURE 4. Light backgrounds used during electrophysiology experiments. Except for the middle-wavelength isolation background, all others mimic natural conditions in mesotrophic waters for the various time periods specified in the figure.

responses in laboratory experiments (transformed similarly) to judge whether polarized light vision, in terms of required intensity, could occur in nature. The second requirement is that the degree of polarization be sufficiently high for the animal to distinguish E-max from unpolarized light, or light polarized in a different orientation (any other E-vector). To calculate the degree of polarization (per cent (%) polarization), two scans in the E-max and E-min planes were conducted for each direction of observation (the E-min plane is the plane of least polarization, and is oriented perpendicular to the E-max plane; Table 1).

As an index to classify the waters studied, we measured chlorophyll concentrations in triplicated samples (Jeffrey & Humphrey, 1975; Table 2). All mathematical analyses in this section used Li-Cor software and the Statistical Analysis System (SAS, version 5).

The visual system of young rainbow trout

Once the properties of the light field in meso-eutrophic waters had been described, the next endeavour was to determine the visual characteristics of the animal under natural light settings. To do this we mimicked the spectral backgrounds found in nature in the laboratory and measured electrophysiologically (as described below) the responses of the animal to spectral stimuli that were either polarized or unpolarized. These experiments permitted us to determine the polarization and spectral sensitivities of the animal for particular spectral background radiances (Fig. 4).

Optical set-up for electrophysiological recordings. The electrophysiological procedure used in these experiments has been described elsewhere [Beaudet *et al.*, 1993; Novales Flamarique & Hawryshyn, 1996; Fig. 5(A)]. In summary, the optic tectum of an anaesthetized fish is surgically exposed and a teflon coated electrode with exposed silver tip is inserted antero-ventrally
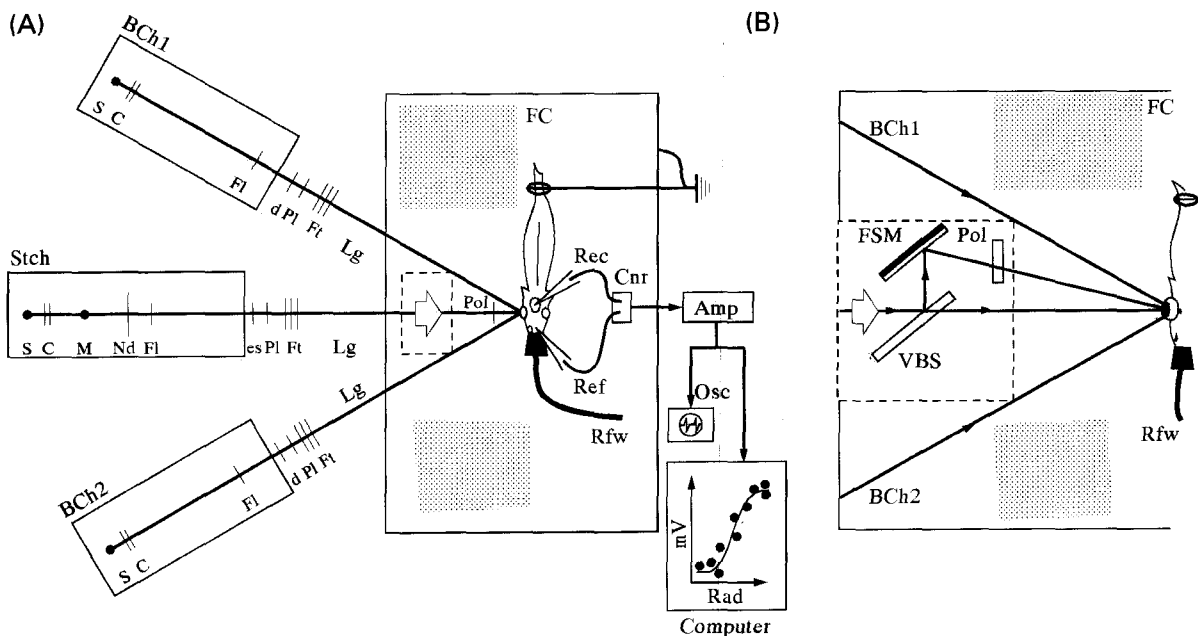
FIGURE 5. (A) Electrophysiology rig: S, light source; C, condenser lens; M, monochrometer; Nd, neutral density wedge; Fl, field lens; d, diaphragm; Pl, projection lens; es, electronic shutter; Ft, filter tray; Lg, light guide; Pol, HNP'B polarizer (light passes through a diffuser just prior to the polarizer); FC, Faraday cage; Rec, recording electrode; Ref, reference electrode; Rfw, respiration flow-through water system; Cnr, common noise rejection unit; Amp, amplifier; Osc, oscilloscope; BCh1, BCh2, background light channels 1 and 2; Stch, stimulus channel. Computer shows a typical amplitude response vs radiance curve. (B) Per cent Pol measurements addition: VBS, variable density beam splitter; FSM, front surface mirror.

through the optic tectum into the optic nerve. Two background channels control the energy distribution illuminating the fish's eye, and a stimulus channel delivers the wavelength and intensity of the stimulus. The stimulus channel is projected onto the central region of the eye (and the retina) where the two background channels overlap as much as possible (nonetheless, adaptation in this set-up is probably due mostly to overlapping horizontal cell dendritic fields). By increasing the intensity of the stimulus for a given wavelength, a curve of response intensity (in μV vs intensity can be generated. A third degree polynomial is then fitted to this curve. Following this, a criterion voltage potential is chosen that meets two conditions: (1) it is as close as possible to the threshold voltage that first evokes a response; and (2) it must lie within the linear part of the intensity–response curve for all wavelengths (or E-vector positions) tested (this ensures predictable and repeatable values). The spectral sensitivity of the animal is defined as the inverse of the intensity value required to reach the criterion response level. This procedure is carried out for selected wavelengths across the spectrum producing a spectral sensitivity curve. Polarization sensitivity curves are obtained similarly, except that the light stimulus passes through a polarizer before reaching the fish's eye. For a specific wavelength during the experiment, the E-max of the light can be changed by rotating the polarizer [Fig. 5(A)].

To measure per cent polarization levels of the light source required for detection by rainbow trout, the optical set-up described above was altered [Fig. 5(B)]. The stimulus light was now split into two components using a variable density beam splitter (Edmund Scientific). The reflected component bounced off a front surface mirror and passed through a rotatable polarizer before reaching the fish's eye. The transmitted component went directly to the fish's eye. Both rays were positioned to overlap as closely as possible the central region of the eye (retina). The ratio of transmitted to reflected energies was altered by changing the position along the length of the beam splitter upon which the light from the source was incident. Because polarized light is produced by reflection from dielectric surfaces (Hecht & Zajac, 1974; Wolff, 1994), the percentage of polarized light for the two polarizer angles tested in this experiment (0 and 90 deg) was calculated from combined measurements from the two components of the stimulus channel. Following measurements of E-max and E-min for the two optical paths individually at the level of the fish's eye, the total % polarization was calculated as:

$$\frac{(\text{E-max}_{mir} + \text{E-max}_{bs} - \text{E-min}_{bs})}{(\text{E-max}_{mir} + \text{E-max}_{bs} + \text{E-min}_{bs})}.$$

In this expression "bs" refers to light coming from the beam splitter, while "mir" is light reflected from the front-surface mirror. The difference in per cent polarization for the two polarizer angles tested was less than 6% for total polarization values above 52% (a difference less than 10% is not considered significant in many engineering applications). Continuous readings from the two optical paths for a given beam splitter position did not reveal differences in energy for the polarization components with time.

Electrophysiological experiments and treatment of data. We conducted three types of experiments on rainbow trout to determine the visual performance of this species under natural light settings. First, we measured the spectral sensitivities of the animal under midday, evening and crepuscular illumination (Fig. 4). The simplex algorithm (Caceci & Cacheris, 1984) was used to fit template-derived pigment absorption values (Fig. 3; Bernard, 1987) according to the general pseudo-pigment equation $R = (\Sigma k_i A^P_i(\lambda))^{1/p}$ (Sirovich & Abramov, 1977), where R is the response curve amplitude at a given wavelength λ, $A_i(\lambda)$ is the absorbance of pigment i at light of wavelength λ, k_i are the coupling constants derived from the fit to the data, and p is an exponent resulting from the mathematical requirement that the function describing the spectral sensitivity curve be differentiable at the origin (Sirovich & Abramov, 1977). The k_i parameters obtained indicate which photoreceptor mechanisms are most active at different times of the day. The λ-max values for generating the pigment absorption spectra from the nomogram have been obtained microspectrophotometrically for rainbow trout (Hawryshyn & Hárosi, 1994). These are 365 nm (UV), 434 nm (short), 531 nm (middle) and 576 nm (long wavelength mechanism). We then generated polarization sensitivity curves under crepuscular conditions, since it is at these times of the day that % polarization was highest in nature (see results later, Fig. 7), and fish activity seems to be at its peak (Johnson & Groot, 1963). Lastly we changed the % polarization of a 520 nm light stimulus to determine the minimum polarization levels required by the fish to detect E-max. We chose 520 nm for these experiments because it approaches the maximum wavelength penetration in meso-eutrophic waters (Novales Flamarique & Hawryshyn, 1993), and is within the absorption spectrum of the short, middle and long wavelength cone mechanisms of rainbow trout. Lack of energy from our Xenon lamp source at 400 nm (after optical reflections) did not permit us to conduct experiments within the UV cone photoreceptor absorption range. However, behavioral, electrophysiological and psychophysical experiments suggest that the minimum % polarization values should be similar for all the mechanisms, and lowest for the middle wavelength one (Hawryshyn & Bolger, 1990; Hawryshyn, 1991; Parkyn & Hawryshyn, 1993, so we are studying the best case scenario). Furthermore, under white light backgrounds of moderate intensity, the "W"-function visual response obtained spans a similar sensitivity range to the isolated responses from either middle- or long-wavelength mechanisms (Parkyn & Hawryshyn, 1993; Coughlin & Hawryshyn, 1995). This does not suggest higher sensitivities to % polarization (i.e., lower detection thresholds) when more than one cone mechanism is acting, as is the case in nature.
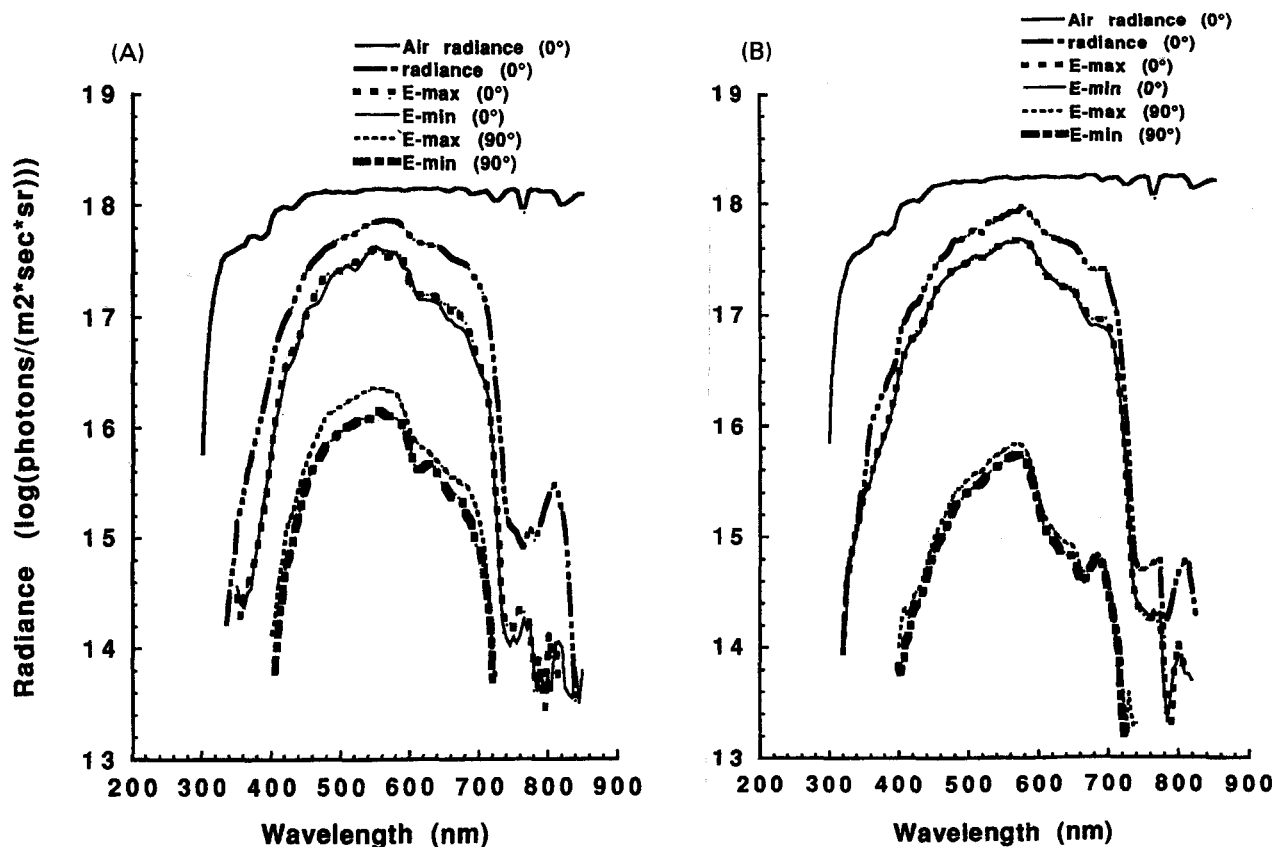
FIGURE 6. Spectral characteristics of the polarized light field at 4 m depth in (A) Lake Cowichan (J = 60°42', %Pol$_{tot}$ = 29.2); and (B) Ogden Point Breakwater (J = 56°28', %Pol$_{tot}$ = 26.4). Highest %Pol in the UV part of the spectrum (32 and 35%, respectively). The zenith angle for each scan is in parentheses and E-max is always the highest curve for any given pair of zenith polarization scans.

All handling and use of animals was in accordance with the guidelines set by the Canadian Council for Animal Care.

RESULTS AND DISCUSSION

General features of the underwater polarized light field

To describe the polarized light field at a specific depth, time of day and for a specific set of atmospheric and water conditions, one must determine how E-max, total energy and per cent polarization vary with direction of observation. We will deal with these questions by studying the polarized light field at 4 m depth under cloudless skies. Then we shall investigate the effects of depth and different atmospheric conditions. For comparison, we will also present spectral radiance measurements under the same light regimes.

In general, the ratio of total radiance to the corresponding light intensities in either the E-max or E-min planes on sunny days is at least 1.5 (Fig. 6). The distribution of energy across the spectrum changes during the course of the day with proportionately more short wavelength photons contributing to the total spectrum during crepuscular periods (Novales Flamarique et al., 1992; Loew & McFarland, 1990). This, in turn, changes the

shape of the E-max and E-min functions in a similar fashion (Fig. 7).

The per cent of polarized light in the plane of E-max is a function of the direction of propagation of the incident sunlight and the direction of observation of the spectroradiometer sensor (see also Timofeeva, 1962, 1974). The direction of sunlight is mostly dependent on the elevation of the sun, while the direction of observation depends both on the azimuth angle φ and the zenith angle θ. The percentage of polarized light changes with azimuth reaching the two highest maxima at θs near 90 and 270 deg in the plane perpendicular to that of the sun [Fig. 8(A)]. The appearance of these maxima can also be observed by scanning all azimuths in a horizontal plane [Fig. 8(B); Ivanoff & Waterman, 1958; Timofeeva, 1974].

Assuming perfect Rayleigh scattering, it can be geometrically derived that the highest % polarization for any direction of observation is given by: $\tan(\theta) = -\cot\text{an}(r)/\cos(\varphi)$ (Appendix), where r is the angle of refraction at the air–water interface. The slight disagreement between angles predicted by this formula and those observed in the field demonstrates that Rayleigh's formula is only an approximation (although a good one) of the scattering taking place in mesoeutrophic waters. Timofeeva (1974) derived the following empirical formula based on laboratory obser-
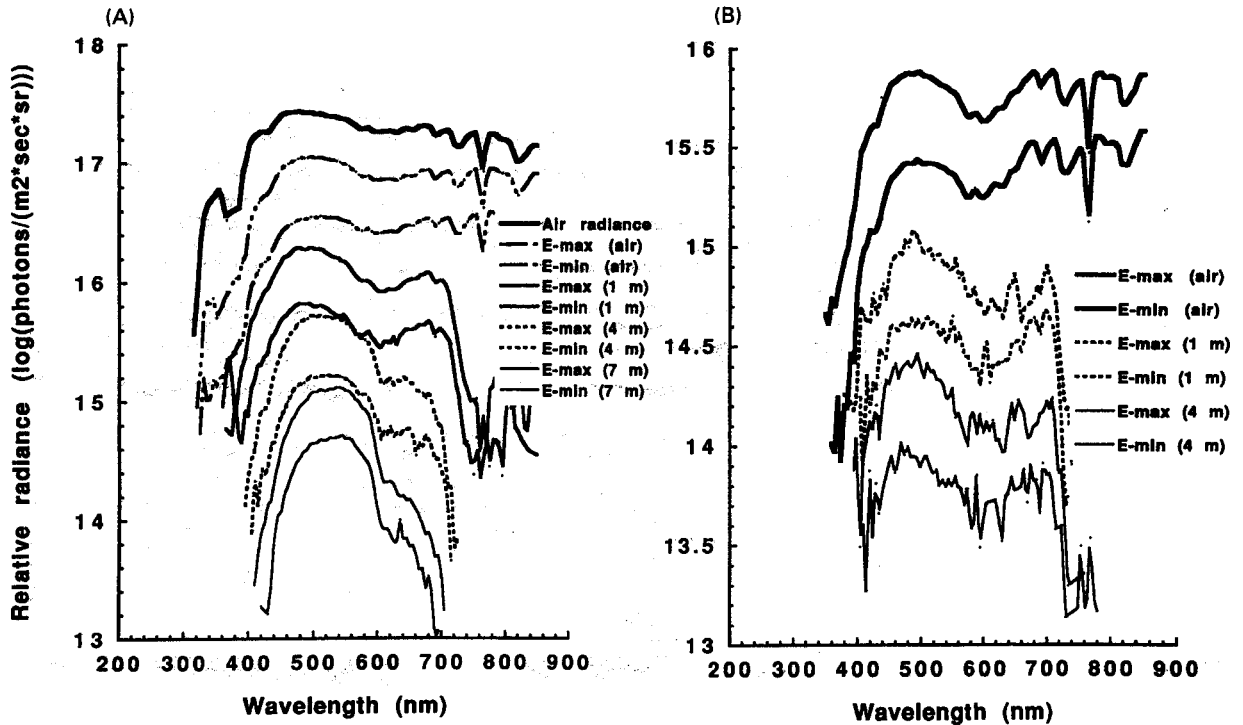
FIGURE 7. Spectral characteristics of the radiance and polarized light fields during dusk in (A) Lake Cowichan (sun just above the horizon); and(B) Ogden Point Breakwater (sun just below the horizon, sunset at 21:02 hr Pacific Standard Time). Per cent Pol_{tot} are 74.2% (air), 65.4% (1 m), 63% (4 m), 52.3% (7 m) (Lake Cowichan), 72.7% (air), 67.2% (1 m), 65.4% (4 m) (Ogden Point Breakwater). Radiance is always the highest in air and diminishes with depth. E-max, E-min curves for a given depth have the same trace but E-max is always the highest. For clarity, 1 log unit was added to all air and 1 m scans in (A), and 0.5 log unit was added to the 4 m scans. In (B), 0.5 log unit was added to the air and 1 m scans.
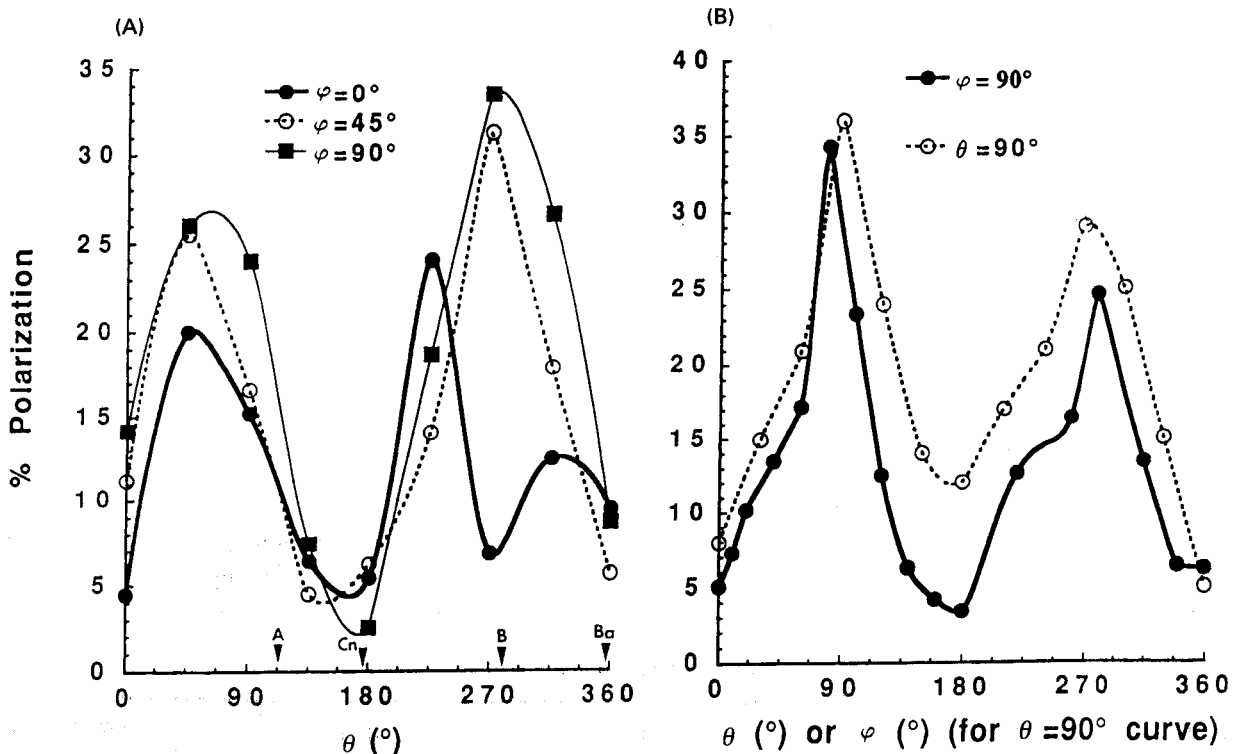
FIGURE 8. (A) Per cent Pol_{tot} as a function of azimuth and zenith angle in Ogden Point Breakwater (4 m depth, J = 43°32′). Arrows indicate approximate position of submarine neutral points (A = Arago, B = Brewster, Ba = Babinet, Cn = "close to nadir"). (B) Per cent Pol_{tot} in the plane perpendicular to the sun and as a function of azimuth in Lake Cowichan (J = 56°33′).
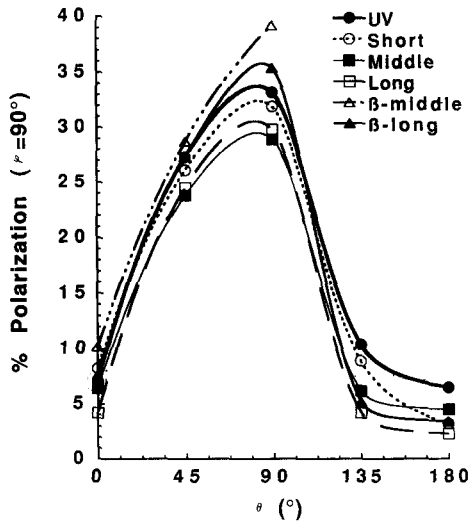
FIGURE 9. Per cent Pol for different parts of the spectrum as a function of zenith angle (Lake Cowichan, J = 64°24′, 7 July 1993). Results are similar for Ogden Point Breakwater location.
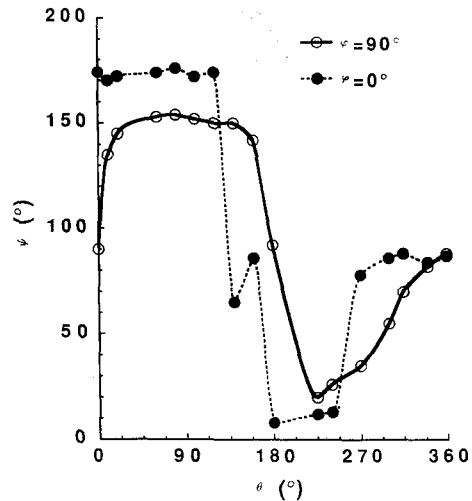

FIGURE 10. Angle of E-max as a function of azimuth and zenith angle. The E-max value for $\theta = 360$ deg must in reality correspond to a zenith angle slightly smaller than 360 deg (Ψ at $\theta = 360$ deg should be equal to Ψ at $\theta = 0$ deg).

vations to predict the same polarization maxima: $\cos\theta(\max) = -\sin 98 \deg*\sin J*\cos\varphi + \cos 98 \deg*\cos J$. More precise equations than those derived using Rayleigh's theory or empirical curve fittings would require the application of Mie's scattering theory to light impinging on an ensemble of particles possessing the range of geometries, sizes and indices of refraction representative of the waters studied (e.g. Zaneveld *et al.*, 1974). Furthermore, the effect of anisotropy and multiple scattering would have to be accounted for (Plass *et al.*, 1975; Marshall & Smith, 1990). Such analyses, however, are more complicated (Van de Hulst, 1957) and do not provide significant additional insight into distributions of light important for visual processes (Wehner, 1983).

As may be inferred by the dispersion and absorption coefficients of light, wavelengths that penetrate most through the media are also the least polarized (% polarization increases with increasing absorption and decreasing dispersion; Timofeeva, 1961). Accordingly, middle wavelength light, which penetrates most in the waters examined, exhibits the lowest degree of polarization, while UV and short wavelengths show the highest percentages (Fig. 9). During the day the highest % polarizations could reach 35%, while during crepuscular periods these values were significantly higher (Fig. 7 legend). These increases during dawn and dusk and the spectral changes observed are due primarily to enhanced scattering but also to airglow phenomena. Indeed, the crepuscular (or twilight) sky is characterized by electronic transitions of atoms and molecules resulting in emission bands at various visible wavelengths (Craig, 1965). Oxygen atoms emit a dual "line" in the red part of the spectrum at 630 and 636.4 nm, contributing to the observed "red" sunsets. However, the strongest emission bands are the product of N^{2+} transitions and occur in the UV-A ($\lambda = 391.4$ nm) and in the blue ($\lambda = 427.8$ nm) parts of the spectrum (Craig, 1965), which would explain the shifts towards shorter wavelengths during twilight.

The observed increases in underwater polarization at these times most likely result from sky polarization. However, changes in the water column (biotic and chemical) may also influence polarization levels by secondary scattering of sky polarized light.

We observed two peculiarities in % polarization throughout the study period. The first occurred during measurements in directions near that of the sun's refracted rays and in the antisun direction. At these angles the diver could not detect a clear E-max. Results in these directions are, therefore, best approximations based on trends followed by nearby points. Previous studies have shown that the E-max vector in these directions can lie in any plane (even in the scattering plane, from which the term "negative zones of polarization" occurring between neutral points where % polarization is zero; Timofeeva, 1969, 1974). Secondly, a few measurements showed 25% polarization levels when scanning reflected light from the silty ocean/lake floor. Such levels of polarization have also been observed using dark sandy substrates in laboratory studies (Chen & Nagaraja Rao, 1968). The values increased further if turbidity was created by resuspending the very fine particles that constituted the bottom of the lake/ocean.

The plane of maximum polarization (E-max) also varies with θ and φ (Fig. 10). Except for directions near the sun and antisun points, E-max can be approximated to be perpendicular to the plane comprising the direction of the incident light, the observer (spectroradiometer sensor) and the point of observation. In the case of crepuscular measurements (the sun being just below the horizon), the E-max angle Ψ (measured with respect to the horizontal, Fig. 1) is always close to 0 deg and % polarization is maximum at $\theta = 0$ deg. This follows from the fact that the incident light on the ocean is already partially polarized and that subsequent secondary polarization by Rayleigh-type particles in the ocean should not alter the maximum E-vector direction (see scattering
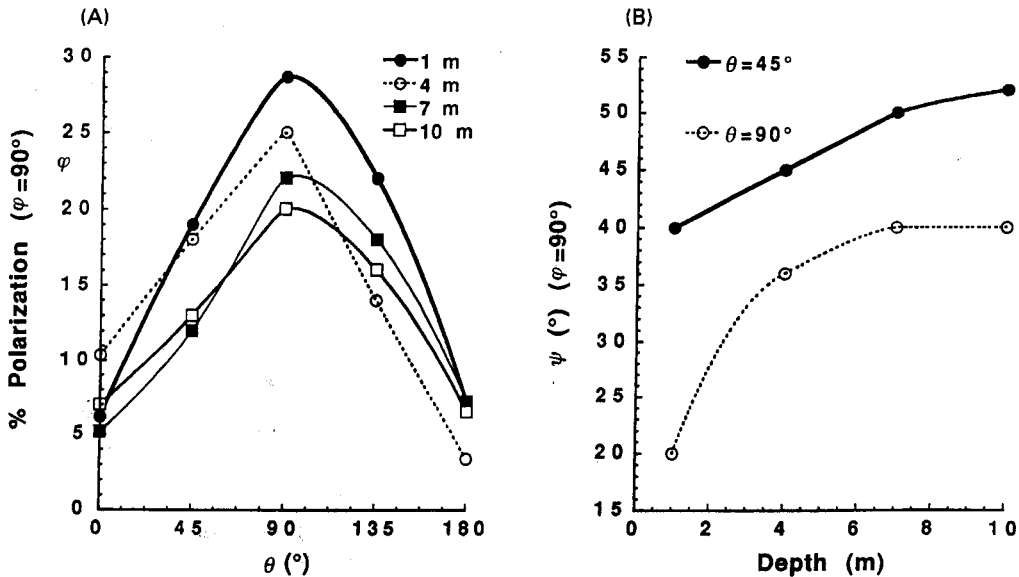
FIGURE 11. (A) Per cent Pol as a function of depth under cloudless skies in Lake Cowichan (J = 56°44′). Reflected light from the lake's bottom may have caused the higher than expected % polarizations at higher zenith angles. (B) Angle of E-max as a function of depth for two zenith angles.
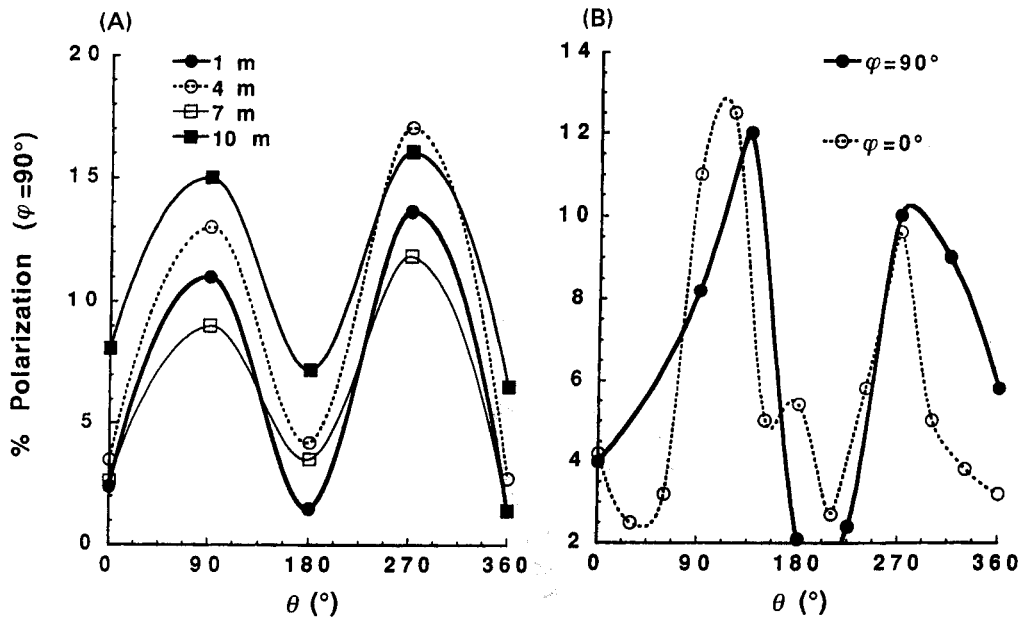

FIGURE 12. (A) Per cent Pol under slight changing overcast (cirrus clouds); and (B) under heavy overcast (grey cumulus clouds), in Ogden Point Breakwater.

diagrams in Hecht & Zajac, 1974). It is worth noticing that by being able to detect these variations in Ψ, an observer is able to tell, regardless of the radiance distribution, the azimuth and elevation of the sun. An expression to predict Ψ from other angles in Fig. 1 was given by Timofeeva (1969). Another way to predict the position of the sun would be to be sensitive to variations in spatial % polarization.

Changes in polarization with depth and overcast skies

Previous studies have shown that the degree of polarization decreases with depth, and reaches a constant maximum at $\theta = 90$ deg, when the radiance distribution

no longer varies with direction of observation (Ivanoff & Waterman, 1958; Timofeeva, 1969). This asymptotic radiance distribution is a function of the optical properties of the medium (Timofeeva, 1969) and has been shown to vary from 40 to 50 m (Ivanoff & Waterman, 1958) to 200 m (Waterman, 1955) in very clear waters. Our measurements by comparison were carried out at shallower depths; however, they also show decreases in photon flux, and % polarization with depth in some directions [Fig. 11(A), $\theta = 90$ deg; see also Novales Flamarique & Hawryshyn, 1993]. Percent polarizations vary slightly, with maxima tending to be found at higher zenith angles with depth (Timofeeva, 1962). E-max
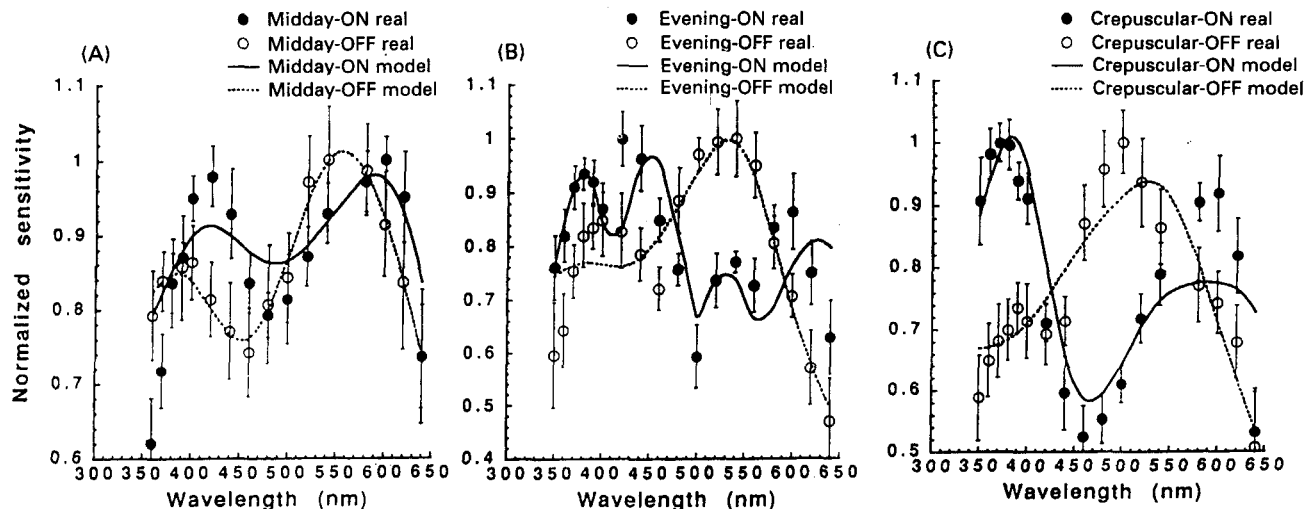
FIGURE 13. Compound Action Potential (CAP) responses from the optic nerve of rainbow trout with the animal adapted to different light intensity backgrounds: (A) midday; (B) evening; (C) crepuscular. Each data point was divided by the inverse of the values at λ-max and the data normalized to obtain the curves shown. The λ-max values (in nm) and associated radiance thresholds in log (cm^2*sec*sr/photons) are as follows: Midday-ON (600 nm, -13.46), Midday-OFF (540, -13.8), Evening-ON (420, -12.81), Evening-OFF (540, -12.87), Crepuscular-ON (380, -12.4), Crepuscular-OFF (500, -13.52). See Table 3 for simplex parameters. $n = 4$ for each curve, bars represent standard errors of the means.

TABLE 3. Simplex parameters for best fits to CAP recordings

Response curve	K (UV)	K (short)	K (middle)	K (long)	p	SS
Midday-ON	0.002	0.161	0.118	0.844	0.187	0.064
Midday-OFF	0.147	0.008	0.547	0.657	0.814	0.004
Evening-ON	0.067	0.271	0.004	0.009	40.65	0.118
Evening-OFF	0.156	0.197	0.826	0.304	1.47	0.066
Crepuscular-ON	0.626	0.004	0.34	0.611	1.429	0.105
Crepuscular-OFF	0	0.243	0.638	0.457	1.103	0.044

SS, sum of squares from the best fit to the data.

distributions also vary as downwelling incident light gradually loses its directionality (becoming more vertical) and multiple scattering increases [Fig. 11(B)]. Perhaps the most important effect in terms of energy is the rapid attenuation of wavelengths below 400 nm and above 700 nm, and the presence of a peak in middle wavelengths as depth increases (Fig. 6; Novales Flamarique & Hawryshyn, 1993).

Although spectral irradiance measurements have indicated differences in intensity with direction of observation under slight cloud cover (Novales Flamarique & Hawryshyn, 1993), polarized light measurements near the surface under similar conditions show very small polarization levels [Fig. 12(A)]. It would appear that the intensity of light that maintains its directionality through the cloud layer is insufficient to create high levels of polarization near the ocean surface. The traces of sun directionality still detectable under light cloud cover are lost under heavy overcast, but the distribution of polarized light still peaks near the horizontal [Fig. 12(B)]. In this case multiple Mie-scattering by water droplets in the atmosphere could be diffusing the light reaching the ocean resulting in mostly vertical downwelling light at the water surface.

Visual responses of rainbow trout under natural light settings

Although the model fit was not always very accurate (possibly due to inaccuracy of the polynomial template, especially in the β band absorbing regions), the fits show a progression of increased activation of the UV cone mechanism towards crepuscular periods for the ON response pathway (Fig. 13, Table 3). During bright light conditions [Fig. 13(A)], the ON response is dominated by the short and long wavelength mechanisms, with a prominent OFF response in the middle to long wavelengths. The OFF response is dominated by the middle wavelength mechanism under moderate light levels [Fig. 13(B)], but the ON-response is now a combination of all the cone mechanisms. In particular, the UV peak starts being noticeable and a middle wavelength mechanism is also present. As the levels of background light diminish towards the crepuscular condition, only the UV and long wavelength mechanisms are major components of the ON response [Fig. 13(C)]. The OFF response is still dominated by middle wavelength mechanism input, but a smaller contribution now arises from the long wavelength mechanism.
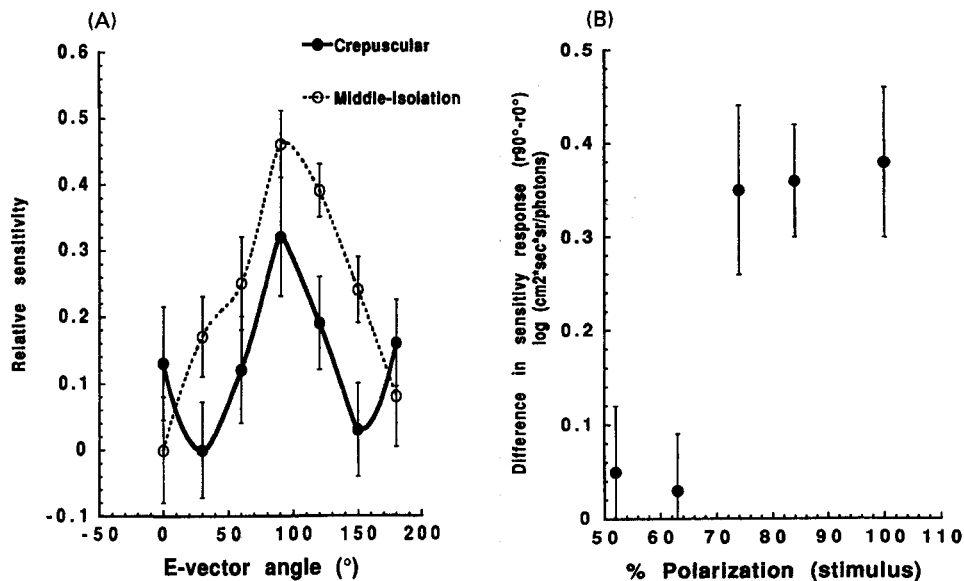
Under crepuscular background conditions, rainbow

FIGURE 14. (A) Polarization responses under crepuscular, and middle wavelength isolating backgrounds. The 0 deg E-vector angle (polarizer position) corresponds to light vibrating in the plane vertical to the long axis of the fish. One fish did not exhibit polarization sensitivity, perhaps due to the placement of the electrode (i.e., not all optic nerve fibres may carry polarization information). This fish was discarded from the analysis. (B) Difference response from the 90 and 0 deg polarizer positions under middle wavelength isolation conditions. $n = 4$ for each curve, bars are standard errors of the means.

trout exhibits a "W"-shaped polarization sensitivity function with local maxima at 0, 90 and 180 deg using a 400 nm stimulus [Fig. 14(A)]. When the middle wavelength mechanism is isolated, the response to polarized light changes to a one-peak maximum at 90 deg [Fig. 14(A), see also Parkyn & Hawryshyn, 1993]. If the fish is then tested for differences in the responses between the 0 and 90 deg E-vector conditions while varying the degree of incident polarized light, no significant difference is found below 72% [Fig. 14(B)]. Polarization sensitivity is therefore lost somewhere between 63 and 72%.

Conclusion: Can underwater polarized light-mediated vision occur in nature?

To answer this question, we must go back to the polarized light measurements and search for time periods when the levels of radiance and % polarization are sufficient to stimulate fish polarization detectors. The measurements point towards crepuscular time periods and only near the water surface (<7 m, Fig. 7). Only during these light conditions can the % polarization attain 67%, and the polarized light energy in the E-max plane be sufficient to stimulate the cone photoreceptors [the regressions showed the onset of the response to start between -14 and -15 $\log(m^2/(photons*sec*sr))$, Fig. 15].

Although the method used to determine polarization perception thresholds was based on optic nerve recordings, other studies using different protocols also support our results. For instance, Heart Rate Associated (HRA) experiments which evaluate the response of the entire animal by monitoring changes in heart rate (Hawryshyn & McFarland, 1987; Cameron & Pugh, 1991) show maxi-
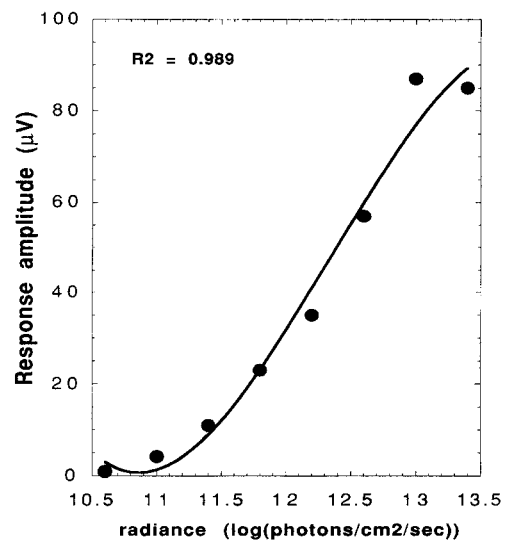

FIGURE 15. Characteristic amplitude response curve obtained durin; the % polarization experiments. Note that the fish starts responding t(radiance stimuli of about $10^{10.5}$ [photons/($cm^2*sec*sr$)]. Such respons(curves can also shift towards higher radiances (1–2 log units, depending on the intrinsic sensitivity (physiology) of the fish.

mum sensitivities around -13 $\log(m^2/(sec*photons*sr))$ (unpubl. data). Such sensitivities are at most one log unit above those observed electrophysiologically. In terms of intensity, this would only change the threshold depth for polarized light perception by a few meters in the waters studied. However, because the amount of polarization at 7 m is below the threshold value for perception in terms of % polarized light (see Fig. 7), the conclusions reached here would be unaltered. Behavioral studies also support our results. Orientation experiments in tanks using rainbow trout show that the animal is unable to orient to the E-max of polarized light when the

light is 65% polarized or less (Hawryshyn & Bolger, 1990). In addition, orientation experiments with sockeye salmon performed at different times of the day in tanks with a view of the sky show major orientation changes only at dusk. Only during this time period (as opposed to midday and afternoon), do the fish change their swimming orientation with respect to the position of a polarizer filter covering the tank (Groot, 1965). Observations during migratory periods (times when the fish could be using polarized light cues for orientation) show peaks in activity at dawn and dusk (Johnson & Groot, 1963). Furthermore, the fish are found near the surface during these time periods (Scarsbrook et al., 1978; Groot, 1965).

It is noteworthy that Horváth and Varjú's (1995) model of the refraction–polarization pattern of skylight at the air–water interface also shows high % polarization values at crepuscular periods. There are two observations that explain this agreement: (1) polarization measurements during crepuscular periods are dominated by sky-created polarized light, and the maximum band of polarized light lies in the zenith direction; (2) light levels are low during crepuscular periods (hence restricted to near the water surface) and the waves were relatively small during these measurements (~ 30–50 cm peak to trough amplitude).

Our spectral sensitivity results suggest that polarization sensitivity may be achieved by the ON response of the UV and long wavelength mechanisms alone [Fig. 13(C)]. These two mechanisms exhibit opposite polarization sensitivity in rainbow trout and goldfish (Hawryshyn & McFarland, 1987; Parkyn & Hawryshyn, 1993), and may give rise, through neuronal interactions, to the "W"-shaped curve under white light background conditions. Figure 13(C) also shows the importance of the middle and long wavelength mechanisms to the OFF response under crepuscular times. Interestingly, single unit recordings from the Torus semicircularis of rainbow trout report biphasic polarization units with ON responses in the UV part of the spectrum, and OFF in the long wavelength part, giving rise to a "W" function (Coughlin & Hawryshyn, 1995).

There is only one study, using the green sunfish, Lepomis cyanellus, that reports polarization sensitivity in the long wavelength part of the spectrum alone (Cameron & Pugh, 1991). Our light measurements show that the use of long wavelengths alone for polarization sensitivity is realistic, provided the green sunfish is at least as sensitive as rainbow trout (UV polarization levels are often slightly higher than corresponding long wavelength ones). A neurophysical polarization sensitivity model for fish possessing a UV cone and showing the characteristic photoreceptor opponent curves of rainbow trout has yet to be formulated. However, such a model will have to consider the input of UV cones to the polarization response, as behavioral experiments show that rainbow trout does not orient in experimental tanks without UV light in the stimulus (Hawryshyn & Bolger, 1990), and large trout (having lost most of the UV cones, Beaudet et al., 1993) also fail to orient (Hawryshyn & Bolger, 1990).

The conclusion that fish underwater polarization

sensitivity should be possible only during crepuscular time periods may not be restricted to meso-eutrophic waters (waters with medium to high productivity, see Table 2). In blue oligotrophic waters, where smaller radii particles would create higher Rayleigh-type scattering, maximum % light polarizations nearing only 60% (usually in the mid to low 50s, though) have been reported for daylight hours (Ivanoff & Waterman, 1958; Waterman & Westell, 1956). Unless fish species living in such waters are more sensitive to polarized light than rainbow trout, the conclusion reached in this study should be general. Our polarization sensitivity experiments with open ocean and oligotrophic lake-dwelling temperate species (also living in clear water environments), support the conclusions in this study.

Although the hypotheses are hard to evaluate, it is interesting to speculate on the ecological advantages that sensitivity to polarized light may confer animals in nature. For both terrestrial and aquatic invertebrates, it has been shown that natural polarized light cues can play an important role in orientation (Wehner, 1983; Goddard & Forward, 1991). Similarly, but under laboratory settings, rainbow trout can orient to the E-vector of polarized light (Hawryshyn et al., 1990; Hawryshyn & Bolger, 1990). There are nonetheless two problems that fish are faced with when using this sensory capability in nature: (1) their low sensitivity to per cent polarized light (as compared to the invertebrates, Labhart, 1996); and (2) atmospheric and water factors (e.g. clouds, waves) that readily disrupt any E-vector patterns by concentrating most of the light vertically. Given this combination of impediments, the potential use of E-vector patterns by fish to orient and navigate in nature is most likely restricted to ideal crepuscular light conditions. A less complicated means to orient using polarized light would involve extracting information by responding to the most intense polarized light band alone. Anatomically, this would only require one photoreceptor type sensitive to polarized light coupled to a luminance detector. Observing the position and rotation of this band during clear crepuscular times could give the fish valuable position and time cues during migration. Such a behaviour would nevertheless require the fish to have prior knowledge of the zenith angle of this band at different times and locations in the lake/ocean. However, this could potentially be learned by the animal during its early life displacements.

Yet another possible use for polarization sensitivity in fish is contrast enhancement of underwater targets (Lythgoe & Hemmings, 1967). In particular, the strongly polarized downwelling and sidewelling backgrounds during crepuscular periods may be disrupted by swimming zooplankton, which fish could then easily detect. Furthermore, even under open-ocean waves (which mainly enhance the size of Snell's window; Plass et al., 1975), and may focus the light in highly restricted bands (McFarland & Lowe, 1983), this capability could remain useful.

One remaining possibility is the use of polarized light

to recognize substrates, plants and/or other animals underwater. The source of polarization in this case would arise from reflection off targets, and this polarization need not be restricted to crepuscular periods provided the targets polarize light to levels above the fish's detection threshold. Object recognition by analysis of reflected polarized light has many engineering applications (Wolff, 1987, 1994). For instance, the range of materials from dielectrics to perfect conductors can be classified with reflected polarization cues (Wolff, 1994). Dielectrics usually exhibit radiance(E-max)/radiance(E-min) > 3 for high polarizing angles, which translates into % polarizations >50%. These high values suggest that surface recognition by fish of some underwater dielectric-like targets (e.g. kelp blades, coral mixtures) may be possible through the analysis of reflected polarized light. Such a function could potentially be useful to select territories with optimal substrate composition for the animal's needs.

Whether fish use polarization sensitivity to enhance their foraging, for object recognition, for orientation and/ or as a means of reflective communication still awaits discovery.

REFERENCES

Beaudet, L., Browman, I. & Hawryshyn, C. W. (1993). Optic nerve response and retinal structure in rainbow trout of different sizes. *Vision Research, 33,* 1739–1746.

Bernard, G. D. (1987). Spectral characterization of butterfly L-receptors using extended Dartnall/McNicholl template functions. *Journal of the Optical Society of America A, 2,* 123.

Biggs, W. W. (1984). Li-1800 underwater spectroradiometer instruction manual. Publication no. 8405-0037. LiCor-Inc.

Caceci, M. S. & Cacheris, W. P. (1984). Fitting curves to data, the simplex algorithm is the answer. *Byte, 5,* 340–360.

Cameron, D. A. & Pugh, E. N. Jr. (1991). Double cones as a basis for a new type of polarization vision in vertebrates. *Nature, 353,* 161–164.

Chen, H. & Nagaraja Rao, C. R. (1968). Polarization of light on reflection by some natural surfaces. *British Journal of Applied Physics, 2,* 1191–1200.

Coughlin, D. J. & Hawryshyn, C. W. (1995). A cellular basis for polarized-light vision in rainbow trout. *Journal of Comparative Physiology A, 176,* 261–272.

Craig, R. A. (1965). *The upper atmosphere. Meteorology and physics* (pp. 412–422). New York: Academic Press.

Goddard, S. M. & Forward, R. B. Jr. (1991). The role of the underwater polarized light pattern in sun compass navigation of the grass shrimp *Palaemonetes vulgaris. Journal of Comparative Physiology A, 169,* 479–491.

Govardovskii, V. I. (1976). Comments on the sensitivity hypothesis. *Vision Research, 16,* 1363–1364.

Groot, C. (1965). On the orientation of sockeye salmon (*Oncorhynchus nerka*) during seaward migration out of lakes. *Behaviour (Supplement)* 14, pp. 105–158. Leiden: E. J. Brill.

Hárosi, F. I. (1975). Absorption spectra and linear dichroism of some amphibian photoreceptors. *Journal of General Physiology, 66,* 357–382.

Hawryshyn, C. W. (1991). Light adaptation properties of the ultraviolet-sensitive cone mechanism in comparison to the other receptor mechanisms of goldfish. *Visual Neuroscience, 6,* 293–301.

Hawryshyn, C. W., Arnold, M. G., Bowering, E. & Cole, R. L. (1990). Spatial orientation of rainbow trout to plane-polarized light: the ontogeny of E-vector discrimination and spectral sensitivity characteristics. *Journal of Comparative Physiology A, 166,* 565–574.

Hawryshyn, C. W., Arnold, M. G., Chiasson, D. & Martin, P. C.

(1989). The ontogeny of ultraviolet photosensitivity in rainbow trout (*Salmo gairdneri*). *Visual Neuroscience, 2,* 247–254.

Hawryshyn, C. W. & Bolger, A. E. (1990). Spatial orientation of trout to partially polarized light. *Journal of Comparative Physiology A, 167,* 691–697.

Hawryshyn, C. W. & Hárosi, F. I. (1994). Spectral characteristics of visual pigments in rainbow trout (*Oncorhynchus mykiss*). *Vision Research, 34,* 1385–1392.

Hawryshyn, C. W. & McFarland, W. N. (1987). Cone photoreceptor mechanisms and the detection of polarized light in fish. *Journal of Comparative Physiology A, 160,* 459–465.

Hecht, E. & Zajac, A. (1974). *Optics* (pp. 219–271). Reading, MA: Addison-Wesley.

Horváth, G. & Varjú, D. (1995). Underwater refraction-polarization patterns of skylight perceived by aquatic animals through Snell's window of the flat water surface. *Vision Research, 35,* 1651–1666.

Ivanoff, A. (1974). Polarization measurements in the sea. In Jerlov, N. & Steeman Nielsen, E. (Eds), *Optical aspects of oceanography* (pp. 151–175). New York: Academic Press.

Ivanoff, A. & Waterman, T. H. (1958). Factors, mainly depth and wavelength, affecting the degree of underwater light polarization. *Journal of Marine Research, 16,* 283–307.

Jeffrey, S. W. & Humphrey, G. F. (1975). New spectrophotometric equations for determining chlorophylls a, b, c^1 and c^2 in higher plants, algae and natural phytoplankton. *Biochemie und Physiologie der Pflanzen, 167,* 191–194.

Johnson, W. E. & Groot, C. (1963). Observations on the migration of young sockeye salmon (*Oncorhynchus nerka*) through a large, complex lake system. *Journal Fisheries Research Board of Canada, 20,* 919–934.

Labhart, T. (1988). Polarization-opponent interneurons in the insect visual system. *Nature, 331,* 435–437.

Labhart, T. (1996). How polarization-sensitive interneurones of crickets perform at low degrees of polarization. *Journal of Experimental Biology, 199,* 1967–1975.

Loew, E. R. & McFarland, W. N. (1990). The underwater visual environment. In Douglas, R. & Djamgoz, M. B. A. (Eds), *Vision in fishes* (pp. 1–43). London: Chapman and Hall.

Lythgoe, J. N. & Hemmings, C. C. (1967). Polarized light and underwater vision. *Nature, 213,* 893–894.

Marshall, B. R. & Smith, R. C. (1990). Raman scattering and in-water ocean optical properties. *Applied Optics, 29,* 71–84.

McFarland, W. N. & Lowe, E. R. (1983). Wave-produced changes in underwater light and their relations to vision. *Environmental Biology of Fishes, 8,* 173–184.

Novales Flamarique, I. (1993). Ultraviolet light in the salmonid environment. University of Victoria Masters Thesis, 188 pp.

Novales Flamarique, I. & Hawryshyn, C. W. (1993). Spectral characteristics of salmonid migratory routes from southern Vancouver Island (British Columbia). *Canadian Journal of Fisheries and Aquatic Sciences, 50,* 1706–1776.

Novales Flamarique, I. & Hawryshyn, C. W. (1996). Retinal development and visual sensitivity of young pacific sockeye salmon (*Oncorhynchus nerka*). *Journal of Experimental Biology, 199,* 869–882.

Novales Flamarique, I., Hendry, A. & Hawryshyn, C. W. (1992). The photic environment of a salmonid nursery lake. *Journal of Experimental Biology, 169,* 121–141.

Parkyn, D. C. & Hawryshyn, C. W. (1993). Polarized light sensitivity in rainbow trout (*Oncorhynchus mykiss*): characterization from multiunit ganglion cell responses in the optic nerve fibres. *Journal of Comparative Physiology A, 172,* 493–500.

Plass, G. N., Kattawar, G. W. & Guinn, J. A. Jr. (1975). Radiative transfer in the earth's atmosphere and ocean: influence of ocean waves. *Applied Optics, 14,* 1924–1937.

Rayleigh, L. (1889). On the transmission of light through an atmosphere containing many small particles in suspension, and on the origin of the blue of the sky. *Philosophical Magazine, 47,* 375–384.

Scarsbrook, J. R., Miller, P. L., Hume, J. M. & McDonald, J. (1978). Purse seine catches of sockeye salmon (*Oncorhynchus nerka*) and

other species of fish at Babine lake, British Columbia. Fisheries and Marine Service. Pacific Biological Station, Nanaimo, BC, Canada. Data report 69, 41 pp.

Sirovich, L. & Abramov, I. (1977). Photopigments and pseudopigments. *Vision Research, 17,* 5–16.

Timofeeva, V. A. (1961). On the problem of polarization of light in turbid media. *Izvestiya Geophysics Series, 5,* 766–774.

Timofeeva, V. A. (1962). Spatial distribution of the degree of polarization of natural light in the sea. *Izvestiya Geophysics Series, 12,* 1843–1851.

Timofeeva, V. A. (1969). Plane of vibrations of polarized light in turbid media. *Izvestiya Atmospheric and Oceanic Physics, 5,* 603–607.

Timofeeva, V. A. (1974). Optics of turbid waters (results of laboratory studies). In Jerlov, N. & Steeman Nielsen, E. (Eds), *Optical aspects of oceanography* (pp. 177–218). New York: Academic Press.

Van de Hulst, H. C. (1957). *Light scattering by small particles.* (pp. 114–130). Dover.

von Frisch, K. (1949). Die Polarisation des Himmelslichts als orienterender Faktor bei den Tanzen der Bienen. *Experientia, 5,* 142–148.

Waterman, T. H. (1954). Polarization patterns in submarine illumination. *Science, 120,* 927–932.

Waterman, T. H. (1955). Polarization of scattered sunlight in deep water. In *Papers in marine biology and oceanography* (pp. 426–434). London: Pergamon Press.

Waterman, T. H. (1981). Polarization sensitivity. In Autrum, H. (Ed.), *Handbook of sensory physiology, Vol VII/6B* (pp. 281–469). Berlin, Heidelberg, New York: Springer.

Waterman, T. H. (1984). Natural polarized light and vision. In Ali, M. A. (Ed.), *Photoreceptors and vision in invertebrates* (pp. 63–114). New York: Plenum Press.

Waterman, T. H. & Westell, W. E. (1956). Quantitative effect of the sun's position on submarine light polarization. *Journal of Marine Research, 15,* 149–169.

Wehner, R. (1983). The perception of polarized light. In Cosens, D. J. & Vince-Price, D. (Eds), *The biology of photoreception* (pp. 331–369). Society of Experimental Biology Symposium XXXVI.

Wehner, R. (1989). Neurobiology of polarization vision. *Trends in Neuroscience, 12,* 353–359.

Wolff, L. B. (1987). Surface orientation from polarization images. In Svetkoff, D. J. (Ed.), *Optics, illumination, and image sensing for machine vision II.* Proceedings of the Society of Photo-Optical Instrumentation Engineers, 850, 110–121.

Wolff, L. B. (1994). Polarization camera for computer vision with a beam splitter. *Journal of the Optical Society of America A, 11,* 2935–2945.

Zaneveld, J. R. V., Roach, D. M. & Pak, H. (1974). The determination of the index of refraction of oceanic particulates. *Journal of Geophysical Research, 79,* 4091–4095.
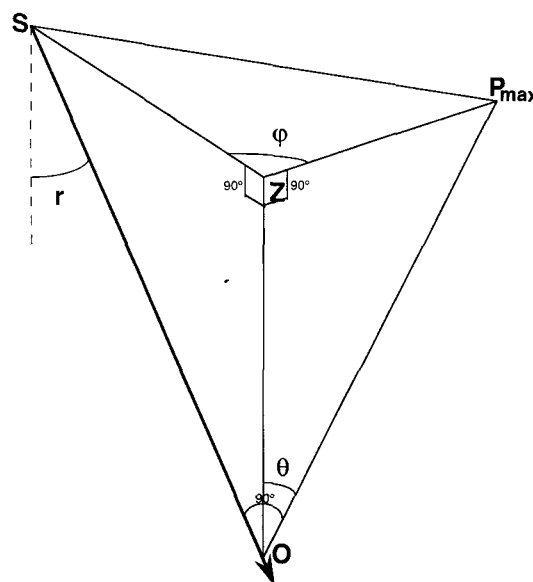
APPENDIX

Consider the following figure in which:

O: particle doing the scattering (the observer, or spectroradiometer sensor looks towards o along the line OP_{max})

S: a point in the refracted ray's direction of propagation, a source

P_{max}: target point, point in space being observed with highest polarization (according to Rayleigh approximation, angle $\angle\,SOPmax = 90\ deg$)

Z: a point in the Zenith direction; on the normal to a flat surface and intercepting o; therefore $\angle\,SZO$ and $\angle\,OZP_{max}$ are right angles. Triangle SZP_{max} is in the x–y plane (see Fig. 2)

φ: azimuth angle, $\angle\,SZP_{max}$

θ: zenith angle, $\angle\,ZOP_{max}$

r: refraction angle (corresponds to the zenith angle of the underwater source)

From this figure, we can write:

$$SP^2_{max} = SZ^2 + ZP^2_{max} - 2(SZ)(ZP_{max})\cos\varphi \tag{A1}$$

$$OP^2_{max} = ZP^2_{max} + ZO^2 \tag{A2}$$

$$SO^2 = ZO^2 + SZ^2 \tag{A3}$$

$$SP^2_{max} = SO^2 + OP^2_{max} \tag{A4}$$

$$ZP_{max} = (ZO)\tan\theta,\ \text{and}\ SZ = (ZO)\tan(r) \tag{A5}$$

Substituting equations (A2) and (A3) into (A4), and (A4) and (A5) into the left and right sides of (A1), respectively, we obtain:

$$ZO^2 + SZ^2 + ZP^2_{max} + ZO^2$$
$$= SZ^2 + ZP^2_{max} - 2(ZO)^2\tan\theta\tan(r)\cos\varphi,$$

$$\Rightarrow 2ZO^2 = -2(ZO)^2\tan\theta\tan(r)\cos\varphi$$

$$\Rightarrow \tan\theta = -1/((\tan(r))\cos\varphi) \Rightarrow \tan\theta = -\cotan(r)/\cos\varphi$$